Interplay of β2* nicotinic receptors and dopamine pathways in the control of spontaneous locomotion

Maria Elena Avale[†], Philippe Faure[†], Stéphanie Pons[†], Patricia Robledo[‡], Thierry Deltheil[§], Denis J. David[§], Alain M. Gardier[§], Rafael Maldonado[‡], Sylvie Granon[†], Jean-Pierre Changeux[†¶], and Uwe Maskos[†¶]

[†]Unité Neurobiologie Intégrative des Systèmes Cholinergiques, Unité de Recherche Associée 2182, Centre National de la Recherche Scientifique, Institut Pasteur, F75724 Paris Cedex 15, France; [‡]Laboratorio de Neurofarmacología, Universidad Pompeu Fabra, Calle Doctor Aiguader 88, 08003 Barcelona, Spain; and [§]Université Paris-Sud, EA 3544 Faculté de Pharmacie, F-92296 Châtenay-Malabry, France

Contributed by Jean-Pierre Changeux, August 5, 2008 (sent for review July 4, 2008)

Acetylcholine (ACh) is a known modulator of the activity of dopaminergic (DAergic) neurons through the stimulation of nicotinic ACh receptors (nAChRs). Yet, the subunit composition and specific location of nAChRs involved in DA-mediated locomotion remain to be established *in vivo*. Mice lacking the β2 subunit of nAChRs (β2KO) display striking hyperactivity in the open field, which suggests an imbalance in DA neurotransmission. Here, we performed the selective gene rescue of functional β2*-nAChRs in either the substantia nigra pars compacta (SNpc) or the ventral tegmental area (VTA) of β2KO mice. SNpc rescued mice displayed normalization of locomotor activity, both in familiar and unfamiliar environments, whereas restoration in the VTA only rescued exploratory behavior. These data demonstrate the dissociation between nigrostriatal and mesolimbic β2*-nAChRs in regulating unique locomotor functions. In addition, the site-directed knockdown of the β2 subunit in the SNpc by RNA interference caused hyperactivity in wild-type mice. These findings highlight the crucial interplay of nAChRs over the DA control of spontaneous locomotion.

dopaminergic systems | gene rescue | lentiviral vector | RNAi

Dopamine (DA) modulates a broad range of brain functions, including motor activity, cognition, and reinforcement (1–3). Midbrain dopaminergic (DAergic) ascending pathways are divided into two major tracts (4) (see Fig. 1*A*). The nigrostriatal pathway projects from the substantia nigra pars compacta (SNpc, A9 cell group) to the dorsal striatum and is primarily involved in the regulation of motor activity. Its degeneration in humans leads to Parkinson's Disease (PD) (1, 5). The mesocorticolimbic tract projects from the ventral tegmental area (VTA, A10) to the nucleus accumbens (NuAcc) of the ventral striatum, limbic areas, and prefrontal cortex (PFC) and is mainly implicated in cognition (3), reward-based learning, and addiction (2).

Several findings indicate a potentially critical role of acetylcholine (ACh) in the regulation of DAergic neuron activity; cholinergic afferents from the pedunculopontine tegmental nucleus (PPTg) and the laterodorsal tegmental nucleus (LDTg) innervate the SNpc and VTA nuclei (6, 7), regulating DA efflux (8–10), whereas cholinergic interneurons present in the ventral and dorsal striatum (11, 12) provide additional anatomical and functional bases for the action of ACh upon DAergic nuclei and terminals (see Fig. 1*A*).

Further evidence suggests that nicotinic ACh receptors containing the β2 subunit (β2*-nAChRs) are implicated in the cholinergic control of DA activity: (*i*) β2*-nAChRs are present in the VTA and SNpc of all mammals (in both the soma of DAergic nuclei and GABAergic interneurons) and at the terminals of DAergic striatal projections (13, 14); (*ii*) somatodendritic β2*-nAChRs regulate the firing patterns of DAergic neurons *in vivo* (15); and (*iii*) striatal cholinergic interneurons locally control DA release through the activation of presynaptic β2*-nAChRs at DAergic terminals (16).

β2*-nAChRs are widely expressed in the mammalian brain and are present in multiple neuronal networks (13, 17, 18). Previous studies with mice lacking β2*-nAChRs (β2KO) have established their involvement in several complex behaviors (19–21), particularly those associated with the reinforcing properties of nicotine, originating from their activity within the VTA (20, 22). However, the functional role of β2*-nAChRs in the control of spontaneous locomotor activity remains to be clarified.

β2KO mice show a striking hyperactivity in the open field (21). We hypothesized that this phenotype is because of an imbalance of DA neurotransmission in the nigrostriatal pathway. To test this hypothesis, we performed a targeted lentiviral genetic rescue of functional β2*-nAChRs in the SNpc of β2KO mice and analyzed the extracellular striatal DA levels, together with the behavioral outcome of this selective restoration. β2*-nAChRs were also restored in the VTA of an independent group of mice for comparison in behavioral experiments. This analysis led to a quantitative model, predicting that the lack of *nigral* β2*-nAChRs would drive the hyperactivity of β2KO mice. The gene rescue approach was then complemented by gene silencing of the β2 subunit in the SNpc of wild-type (WT) mice by RNA interference (RNAi). Together, our results establish a critical role for nigral β2*-nAChRs in the control of DA-dependent spontaneous locomotion.

Results

Genetic rescue of the β2 subunit was obtained by stereotaxic injection of a bicistronic lentiviral expression vector [Fig. 1*B* and supporting information (SI) *Text*] into either the SNpc (*SNpc-RESC*) or the VTA (*VTA-RESC*) of β2KO mice. The lentiviral construct drives the coexpression of the mouse β2 subunit (Fig. 1 *D–F*) and the eGFP reporter gene (Fig. 1*C*). The site of injection was chosen to achieve a restricted transduction of neurons within the SNpc (Fig. 1*C Left* and Fig. S1) or the VTA (Fig. 1*C Right*). The reexpressed β2 subunit, partnered with endogenous α subunits, restored ≈50% of [^{125}I]-epibatidine binding sites at the injection area (Fig. 1*E*) and ≈10% of the sites in its target area in the dorsal striatum (Fig. 1*F*). This finding demonstrates that high-affinity β2*-nAChRs were recovered along the nigrostriatal pathway, as also observed by [^{125}I]-epibatidine autoradiography in sagittal sections (Fig. 1*D*).

Author contributions: M.E.A., J.-P.C., and U.M. designed research; M.E.A., S.P., P.R., T.D., and S.G. performed research; D.J.D. and R.M. contributed new reagents/analytic tools; M.E.A., P.F., A.M.G., S.G., and U.M. analyzed data; and M.E.A., J.-P.C., and U.M. wrote the paper.

The authors declare no conflict of interest.

Freely available online through the PNAS open access option.

¶To whom correspondence may be addressed at: Unité Neurobiologie Intégrative des Systèmes Cholinergiques, Institut Pasteur, 25, rue du Docteur Roux, 75724 Paris Cedex 15, France. E-mail: changeux@pasteur.fr or umaskos@pasteur.fr.

This article contains supporting information online at www.pnas.org/cgi/content/full/0807635105/DCSupplemental.

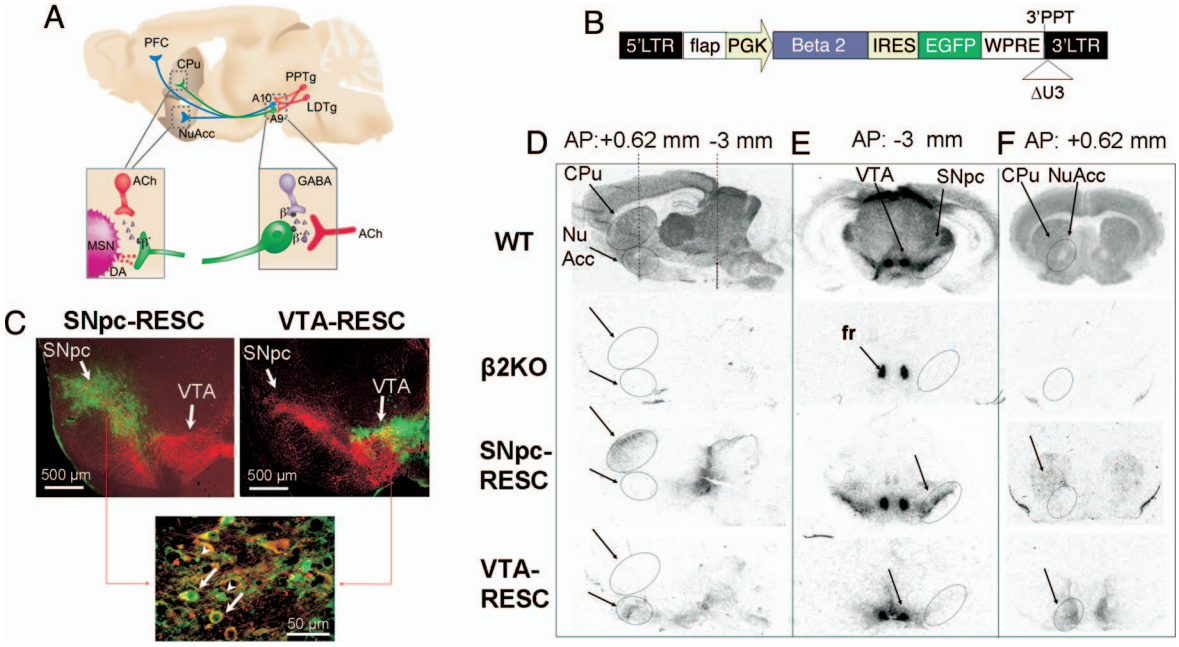

Fig. 1. Lentiviral restoration of functional β2*-nAChRs in the DAergic pathways of β2KO mice. (*A*) Midbrain DA pathways from SNpc (A9; green) and VTA (A10; blue) innervating caudate putamen (CPu) or NuAcc and PFC. Shown in red are cholinergic afferents from LDTg and PPTg to DA nuclei. The magnifications show DA striatal terminal (left), with cholinergic interneurons in red, and cholinergic inputs over DA nuclei and GABA interneuron (right). β*, β2*-nAChRs. (*B*) Map of the bicistronic lentiviral reexpression vector [PGK-β2-Ires-eGFP]. LTR, long terminal repeat; FLAP, sequence comprising central polypurine tract and central termination sequence (see *SI Text*); PGK, mouse phosphoglycerate kinase promoter; beta2, mouse WT β2 nicotinic ACh receptor subunit cDNA; IRES2, internal ribosome entry sequence; eGFP, enhanced green fluorescent protein; WPRE, woodchuck hepatitis B virus posttranscriptional regulatory element; 3′PPT, 3′polypurine tract; ΔU3, deletion of U3 portion of 3′LTR. (*C*) Coronal sections (−3 mm from bregma) showing the site of lentivirus injection in SNpc-RESC (*Left*) and VTA-RESC mice (*Right*). eGFP (green) indicates the virally transduced area and TH (red) stains DA neurons of the SNpc and VTA. Shown in the magnification are lentivirus-transduced DA neurons, showing colocalization of eGFP and TH (arrows), or eGFP-positive non-TH neurons and glial cells (arrowheads). (*D–F*) [^{125}I]-epibatidine autoradiography demonstrating restoration of high-affinity β2*-nAChRs binding sites in SNpc-RESC and VTA-RESC mice. (*D*) Saggital sections (1 mm lateral from the bregma suture). (*E*) Coronal sections at −3 mm from bregma containing the SNpc and VTA [fasciculus retroflexus (fr; arrow) shows non-β2* binding of [^{125}I]-epibatidine]. (*F*) Coronal sections at + 0.62 mm from bregma, showing region-specific reexpression in the CPu projections of SNpc-RESC and in the NuAcc of VTA-RESC mice. Arrows indicate reexpression areas at CPu and NuAcc (*D* and *F*) or at SNpc and VTA (*E*).

Based on previous work (15), we hypothesized that the lack of nigral β2*-nAChRs affects DA release in the dorsal striatum. We thus compared the levels of spontaneous DA release by *in vivo* microdialysis in the dorsal striatum of freely moving mice (Fig. 2 *A* and *B*). Extracellular concentrations of DA under basal conditions, as well as after an injection of saline, were found to be decreased ≈50% in β2KO mice compared with WT animals [WT = 234.9 ± 36.7 vs. KO = 125 ± 50.1 pg/μl (mean ± SEM); mean Δ = 109.9]. After β2*-nAChR reexpression, *SNpc-RESC* mice showed basal levels similar to WT [220.2 ± 39.4 pg/μl (mean ± SEM); one-way ANOVA, group effect $P < 0.05$; followed by Dunnett's post hoc test]. Our data show *in vivo* that

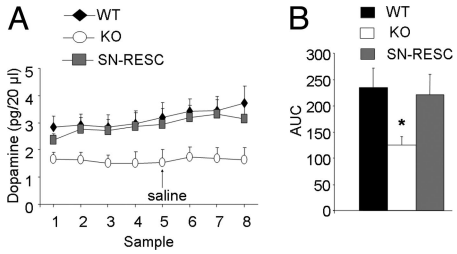

Fig. 2. Nigral β2*-nAChRs control striatal DA release. (*A*) DA extracellular concentrations (pg/20 μl) in the striatum of WT, β2KO, and SNpc-RESC mice under basal conditions (100 min) and after an i.p. injection of saline (0.1 ml/10g, arrow; WT, $n = 11$; KO, $n = 10$; SNpc-RESC, $n = 9$). (*B*) Area under the curve (AUC) values from 20–100 min for basal concentrations of DA in WT, KO, and SNpc-RESC mice. *, $P < 0.05$ (Dunnett vs. WT mice).

mice lacking β2*-nAChRs exhibit decreased levels of striatal DA. This deficit was completely recovered after lentiviral genetic rescue, demonstrating the functional state of the reexpressed β2*-nAChRs. In addition, the restored β2*-nAChRs were able to mediate nicotine-elicited DA release (*SI Text* and Fig. S2).

Having established the efficacy and functionality of the reexpression system, we examined the open-field activity of *SNpc-RESC* compared with *VTA-RESC* mice. Each *RESC* group had two paired control groups, one of WT and the other of β2KO mice, injected in the same structure (SNpc or VTA) with a control lentivirus expressing only the eGFP reporter gene. Mouse trajectories were tracked to determine the total distance traveled and the time spent either in fast or slow movements (see *Methods*). Total distance traveled in the open field was enhanced by ≈40% in KO compared with WT [WT = 15300 ± 703 cm vs. KO = 21397 ± 677 cm (mean ± SEM); mean Δ = 6097, $P < 0.01$] (Fig. 3*A*). Consistent with this hyperactive phenotype, KO mice also spent more time in fast movements [WT = 571 ± 49 vs. KO = 786 ± 33 sec (mean ± SEM); mean Δ = 215, $P < 0.01$] (Fig. 3*B*) and less time in slow movements (WT = 987 ± 27 vs. KO = 702 ± 37 sec; mean Δ = −285, $P < 0.01$) (Fig. 3*C*). In turn, *SNpc-RESC* mice showed a restoration to WT levels of the distance traveled (17015 ± 742 cm) (Fig. 3*A*) and fast movements (622 ± 31 sec) (Fig. 3*B*), whereas the slow movements were not significantly restored and remained comparable to the KO levels (791 ± 40 sec) (Fig. 3*C*). This effect was the opposite of that observed in *VTA-RESC* mice, which displayed distance traveled (19934 ± 648 cm) and fast movement scores (728 ± 21

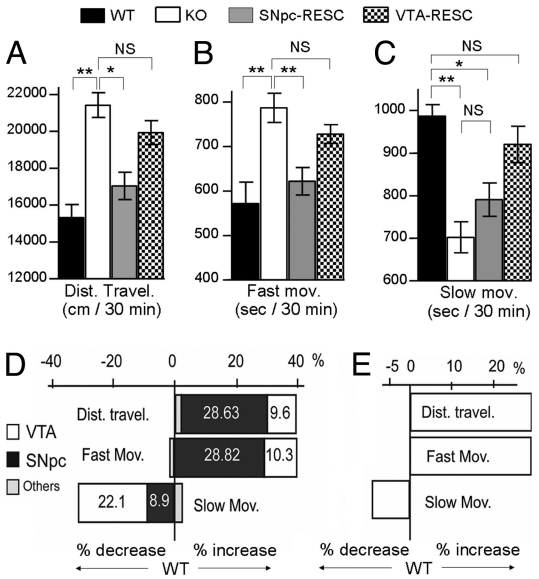

Fig. 3. Quantitative analysis of open-field behavior and its predictions. Total distance traveled (*A*) and time spent in fast (*B*) or slow (*C*) movements during a 30-min session in the open field. *SNpc-RESC* were restored to WT levels of distance traveled and fast, but not slow, movements. *VTA-RESC* showed only restoration of slow movements. One-way ANOVA, followed by Tukey's Multiple Comparison test: WT, $n = 19$; KO, $n = 20$; SNpc-RESC, $n = 12$; VTA-RESC, $n = 10$; *, $P < 0.05$; **, $P < 0.01$. (*D*) Mean percentage of variation in five open-field parameters in β2KO compared with WT (0). Bars indicate decrease or increase in each parameter. The total percentage of variation is indicated in the top line. In each bar the respective contribution of β2*-nAChRs from SNpc, VTA, or other regions is indicated. These values were calculated based on the percentage of restoration of each parameter achieved by the reexpression experiments. (*E*) Predicted variation of open-field parameters in a WT mouse with elimination of β2*-nAChRs in the SNpc, considering the percentage of variation for each parameter according to the values obtained in *D*.

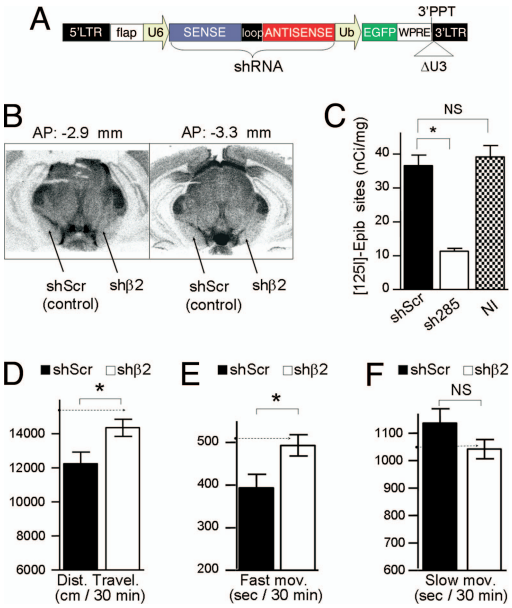

Fig. 4. Silencing of the β2 subunit in the SNpc by a lentivirus-delivered short inhibitory RNA. (*A*) Map of the lentiviral RNAi vectors [U6-shRNA-Ubiq-EGFP], silencing vector (shβ2), or control vector (shScr). U6, polymerase III promoter to drive the transcription of sh shRNAs; sense, shRNA target sequences (see *Methods*); loop, sequence from an endogenous miRNA (5′ GTGAAGCCACAGATG 3′); antisense, complementary to the sense sequence, used to form the sh double strand RNA; Ubiq, human ubiquitin promoter; eGFP, green fluorescent protein. All other regions indicated in the diagram are identical to the reexpression vector in Fig. 1*B*. (*B*) [^{125}I]-epibatidine autoradiography showing decrease in β2*-nAChRs in the SNpc after the injection of shβ2 compared with control side injected with shScr (*Left*, rostral coronal section at −2.9 mm; *Right*, caudal section at −3.3 mm from Bregma). (*C*) Mean values of [^{125}I]-epibatidine binding in SNpc of mice injected with shβ2 or shScr or not injected (NI). Binding was quantified at four consecutive coronal sections per mouse (between −2.9 and −3.3 mm from bregma). One-way ANOVA followed by Tukey's Multiple Comparison test (shβ2, $n = 8$; shScr, $n = 6$; NI, $n = 4$); *, $P < 0.01$. (*D–F*) Behavioral analysis during 30 min in the open field. Shown are the total distance traveled (*D*) and time spent in fast (*E*) or slow (*F*) movements of WT mice bilaterally injected with shScr or shβ2 in the SNpc. In shβ2-injected mice, distance traveled and time in navigation were increased from the shScr group (mean ± SEM; two-tailed Student's *t* test; shβ2, $n = 8$; shScr, $n = 8$; *, $P < 0.05$). Dashed lines indicate the values predicted for the shβ2 group (see Fig. 3*E*).

sec) similar to the KO group (Fig. 3 *A* and *B*), but the slow activity (920 ± 43 sec) was restored to the WT level (Fig. 3*C*).

This clear-cut experimental outcome led us to develop a quantitative predictive model of the localized contribution of β2*-nAChRs to the open-field behaviors. The β2KO locomotor phenotype could be expressed as a percentage of modification of three parameters (from WT values): an average of 40% increase in distance traveled and fast movements and 30% decrease of slow movements. Assuming that a given phenotype results from a linear combination of β2*-nAChR effects in any brain region, the four prototypical phenotypes (WT, β2KO, SNpc-RESC, and VTA-RESC) were used to determine the relative contribution of β2*-nAChRs in the SNpc, the VTA, or other brain areas. Such a decomposition revealed that ≈75% of the increase in distance traveled and time spent in fast movements observed in β2KO mice can be explained by the lack of β2*-nAChRs in the SNpc and <25% by their lack in the VTA (Fig. 3*D*). Based on this model, we calculated the expected variation in these behavioral parameters in an experiment where β2*-nAChRs would be removed only from the SNpc of WT mice. Our model predicts that such a regionally restricted removal would enhance locomotion parameters by 30% from the WT basal level, whereas the slow activity would only be reduced by <10% (Fig. 3*E*).

To test this prediction, we carried out a region-specific knockdown of β2 gene expression in the SNpc of WT mice by a lentivirus-delivered short inhibitory RNA. We developed a silencing lentiviral vector (Fig. 4*A*) expressing a short hairpin (sh) RNA against the β2 subunit (*shβ2*) and a control lentivector expressing a mismatched (scrambled) shRNA sequence (*shScr*), with no silencing effects. The most effective *shβ2* target sequence was chosen after preliminary assays by using different constructs (*SI Text* and Fig. S3). Lentivirus carrying the *shβ2* effectively reduced the expression of β2*-nAChRs in the SNpc as evidenced by a 70% decrease in [^{125}I]-epibatidine-binding sites compared with control *shScr*-injected or noninjected SNpc (Fig. 4 *B* and *C*, *SI Text*, and Fig. S4).

To analyze the behavioral outcomes of the local β2 knockdown, mice were bilaterally injected in the SNpc with either the *shβ2* or the *shScr* lentivirus and were tested in the open field three months after injection (Fig. 4 *D–F*) after a preliminary time-course analysis of the shRNA effect (see *SI Text* and Fig. S5). The shβ2-injected group displayed a significant increase in the total distance traveled [shβ2 = 14181 ± 479 vs. shSCR = 12242 ± 683 cm (mean ± SEM); mean Δ = 1939] (Fig. 4*D*) and in time spent in fast movements [shβ2 = 487 ± 46 vs. shSCR = 393 ± 31 sec (mean ± SEM); mean Δ = 94, $P < 0.05$] (Fig. 4*E*). However, no significant differences were observed in the slow-movements behavior [shβ2 = 1128 ± 47 vs. shSCR = 1048 ± 28 sec (mean ± SEM); mean Δ = 80, *NS*] (Fig. 4*F*), supporting our previous finding that this activity is under the control of β2*-nAChRs in the VTA (22). The experimental data fit well with the values predicted by using the quantitative linear model (Fig. 3*E* and dashed arrows in Fig. 4 *D–F*).

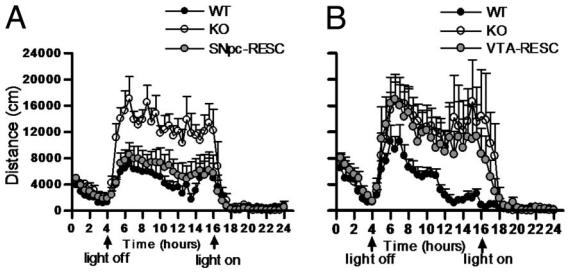

Fig. 5. Nigrostriatal $\beta 2$*-nAChRs modulate nocturnal activity in a familiar environment. Total distance traveled in activity boxes during 24 h (dark phase: 8:00 p.m. to 8:00 a.m.), starting at 3:00 p.m. (*A* and *B*) $\beta 2$KO mice display enhanced motor activity compared with WT mice during the dark phase ($P < 0.01$; repeated measures ANOVA followed by Fisher LSD test). (*A*) SNpc-RESC mice recovered normal (WT) levels of activity during the dark phase (WT, $n = 8$; KO, $n = 8$; SNpc-RESC, $n = 11$). (*B*) VTA-RESC mice activity was similar to the KO group during the whole test (WT, $n = 9$; KO, $n = 11$; VTA-RESC, $n = 9$; scale in *y* axis as in *A*).

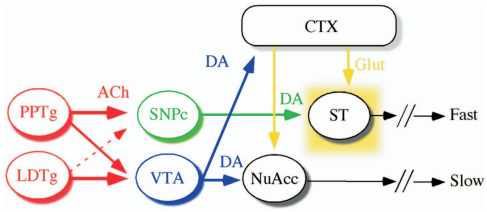

Fig. 6. Endogenous cholinergic control through $\beta 2$*-nAChRs over DA pathways and spontaneous locomotion: a model. Cholinergic afferents (red) from PPTg or LDTg arrive to DA nuclei at VTA and SNpc and control DA release through $\beta 2$*-nAChRs either at the nigrostriatal (green) or mesocorticolimbic (blue) pathways. Glutamatergic corticostriatal inputs (orange) stimulate medium spiny neurons (MSNs) both at dorsal and ventral striatum. DA action at MSNs controls the basal ganglia outputs and the manifestation of fast or slow movements, depending on DA balance between nigrostriatal vs. mesolimbic circuits.

Having observed this critical role of nigrostriatal $\beta 2$*-nAChRs upon open-field activity, we wanted to determine to what extent they were also involved in regulating mouse activity in an environment similar to their home cage (familiar environment). A correlation had previously been established between cholinergic neurotransmission and the circadian rhythm of motor activity (23). We thus recorded the time-course activity of WT, $\beta 2$KO, *SNpc-RESC*, and *VTA-RESC* mice during a complete 24-h cycle in home-cage-like boxes (see *Methods*). The activity of all groups exhibited a similar rhythm; it decreased during the initial light phase, corresponding to the habituation period, followed by an enhancement during the dark phase, which reached the maximal level during the first 4 h of this period (Fig. 5 *A* and *B*). Although the rhythm was not altered in KO mice, they were almost threefold more active than the WT group during the dark phase [WT = 4747 ± 812 vs. KO = 12382 ± 783 (mean ± SEM); mean $\Delta = 7635$, $P < 0.01$]. In rescued mice, nocturnal activity of *SNpc-RESC* was restored to WT levels (6209 ± 969.7) (Fig. 5*A*), whereas *VTA-RESC* mice showed the same activity as the corresponding KO group (11190 ± 720) (Fig. 5*B*), suggesting that normal nocturnal activity is also dependent on the presence of functional nigral $\beta 2$*-nAChRs.

Discussion

Here we analyzed the role of $\beta 2$*-nAChRs in the ascending DA pathways involved in the control of locomotion. Our results establish *in vivo* that nigrostriatal $\beta 2$*-nAChRs are major partners in the cholinergic action on the DA neurons that control locomotion. Combining $\beta 2$KO mice with lentiviral gene delivery, we were able to locally switch on or off the expression of $\beta 2$*-nAChRs restricted to a given DA pathway. In addition to restoring fully functional $\beta 2$*-nAChRs, lentivirus vectors were also efficacious in delivering small inhibitory RNAs to obtain a local knock-down in WT mice, despite the technical difficulties of performing RNAi *in vivo* into the mammalian brain (24).

The data presented here demonstrate that the lack of nigral $\beta 2$*-nAChRs is responsible for the hyperactivity observed in the $\beta 2$KO model. The open-field analysis was used to determine the rate of motor activity in a novel environment, discriminating between fast and slow movements. Our results clearly show that the SNpc and the VTA appear to be involved in different types of motor behavior. Based on previous analysis of this paradigm (21), we postulate that fast movements represent navigatory activity, intended to acquire general information of the arena, whereas slow local movements (exploration) lead to a more precise investigation of the environment and rely on the activation of meso-corticolimbic DA circuits. Indeed, our present results highlight the dissection between motor behavior (distance traveled and fast movements) mainly controlled by nigrostriatal $\beta 2$*-nAChRs, and exploratory behavior (slow movements) that would mobilize $\beta 2$*-nAChRs in the mesolimbic pathway (see Fig. 6 for a simplified model). We were thus able to reproduce the classical dissociation between motor vs. motivational/cognitive DA pathways, specifically addressing the role of $\beta 2$*-nAChRs in these circuits. In our paradigm, however, the analysis of the mesolimbic DA pathway is restricted to the slow movements that mice display in a novel arena; this is an endophenotype that does not necessarily correlate with cognitive performance or motivation in other paradigms and/or species.

Based on our present and previous data (21, 22), we postulate that ACh differentially stimulates $\beta 2$*-nAChRs on DA neurons at either the SNpc or the VTA pathways, giving rise to a transition between fast and slow movements when mice are exposed to a novel open field. The two primary $\beta 2$*-nAChRs present in the SNpc and VTA are $\alpha 4\beta 2$* and $\alpha 6\beta 2$* (14), which mediate the endogenous cholinergic modulation of DA release. Thus, one subtype of α-partners might obviously be involved in the behaviors analyzed here. However, neither $\alpha 4$KO nor $\alpha 6$KO mice showed behavioral differences in the open field (S.G., unpublished data), perhaps because of mutual compensation.

Regarding activity over 24 h, it had been shown previously that ACh levels fluctuate with the light/dark cycle in rodents with a substantial increase at lights out in key regions like the dorsal striatum (23) where the action of ACh on nAChRs would be responsible for behavioral arousal during the dark period. Here we confirmed the involvement of $\beta 2$*-nAChRs in the regulation of spontaneous nocturnal activity by the higher activity scores of $\beta 2$KO mice observed in two independent experiments. Because this phenotype seems to be closely related to the enhanced locomotion of $\beta 2$KOs in the open field, it is tempting to speculate that the same circuits would participate in the manifestation of the two hyperactive phenotypes, both involving nigrostriatal $\beta 2$*-nAChRs. The fact that normal nocturnal activity was restored in *SNpc-RESC* but not in *VTA-RESC* is consistent with this hypothesis. However, the systems regulating 24-h nocturnal hyperactivity are more complex, or at least differentially balanced, than those operating during the open-field test because the specific elimination of $\beta 2$*-nAChRs in the SNpc by RNAi, which effectively enhanced open-field activity (see Fig. 4 *D–F*), failed to affect normal nocturnal behavior (see *SI Text* and Fig. S6).

Our findings of a decreased level of extracellular DA in the striatum of $\beta 2$KO mice that is recovered in SNpc-RESC establish a plausible causal link between the lack of nigral $\beta 2$*-nAChRs and the manifestation of hyperactivity. Although it may seem paradoxical, this phenomenon has been observed before in

rodent models of neonatal partial nigrostriatal DA depletion (25). In that experimental system, as well as in the β2KO, DA is not absent but diminished by ≈50%. In this context, several changes may take place, for example, the hyperstimulation of the corticostriatal tone (26), which could lead to hyperactivity.

Based on the anatomical and electrophysiological evidence available (15, 16), two main check points appear plausible for ACh action over nigrostriatal β2*-nAChRs: the midbrain DA nuclei themselves or their striatal DA terminals (see Fig. 1*A*). Our present data do not exclude a local cholinergic control at the striatal level through presynaptic β2*-nAChRs, which is indeed crucial to control DA release, but we rather consider that the cholinergic inputs arriving from PPTg/LDTg nuclei would activate nigral somatodendritic β2*-nAChRs, serving as a gate that enables DA neurons to respond to the glutamatergic stimulus, which results in burst firing and enhanced DA release (27).

Together, our observations of the key role of β2*-nAChRs in the control of locomotor activity are of prime interest in basal-ganglia-related disorders, particularly those pathological conditions affecting DA activity. For example, cholinergic hyperinnervation at the SNpc was found among the plastic changes observed in the Parkinsonian state (28), triggered to compensate the dramatic loss in DA release. In addition, nicotine exerts a neuroprotective effect on DA neurons (29), and it is tempting to suggest that β2*-nAChRs could be involved in its action. The specific targeting of nigral β2*-nAChRs might thus aid in stimulating the remaining DA neurons in early PD and promoting their long-term survival. On the other hand, DA dysfunction is also widely implicated in ADHD (30), and the β2KO mouse has previously been proposed as a model for this syndrome (31). The use of nicotine in ADHD patients produces a relief similar to standard psychostimulant medications (32). The β2*-nAChRs should therefore be taken into account to both better understand the actions of endogenous ACh under normal and pathological conditions and to design more selective therapeutic cholinergic agents to combat neurological disorders.

Methods

Lentiviral Vectors. Reexpression vectors carrying either β2—IRES–eGFP or only the eGFP sequence under control of the PGK promoter were based on modified pTRIPΔU3, as described previously (ref. 22 and *SI Text*). Lentivirus vectors containing sh RNAs were based on modified pTRIPΔU3, but in this case the expression cassette contains the U6 (*Pol III*) promoter to drive the expression of the selected sh sequence, followed by the ubiquitin promoter and the eGFP sequence (for details on the construction of this vector, see *SI Text*).

shRNA Design. Three sequences of sh RNA to target the mouse β2 subunit gene were designed according to published rules (33) (for details of shRNA design and selection, see *SI Text*). Hairpin sequences were cloned into lentiviral vectors and tested *in vivo* to choose the one with the most efficient gene silencing (see Fig. S3). The following sequences were chosen: target sequence, shB2: 5′ GCCTGAGGATTTCGACAATAT 3′; control sequence, shScr: 5′ GCCAGATTTCTCAGGTGATAA 3′.

Lentivirus Production. Viral particles were generated as described previously (22). Briefly, HEK-293T cells (at 80–85% confluence) were cotransfected with the vector plasmid (either the pTRIPΔU3 [PGK-Beta2-Ires2-EGFP] or the pTRIPΔU3 [U6-shRNA-Ubiq-EGFP]), together with a packaging plasmid (CMVΔ8.9) and an envelope plasmid (CMV-VSVg), by using Lipofectamine Plus (Invitrogen) according to the manufacturer's instructions. Two days after transfection, viral particles were harvested from the supernatant, treated with DNaseI (1/5000; 0.2 μl/ml) and 2 M $MgCl_2$ (1 μl/ml), filtered through 0.45-μm pores and concentrated by ultracentrifugation at 24,000 rpm for 90 min (rotor SW32Ti, Beckman Coulter; $\omega^2 t = 3.2 \times 10^{10}$ rad^2/sec). Viruses were stored in 10-μl aliquots at −80°C. Viral titers were determined by quantification of the p24 capsid protein using an HIV-1 p24 antigen immunoassay (Beckman Coulter). As all lentivectors contained the eGFP sequence, transfecting units were estimated by Fluorescence Activated Cell Sorting (FACS) after the infection of HEK-293T cells with increasing doses of each viral production. Immediately before stereotaxic injections, lentiviruses were diluted in PBS to achieve a dose of injection of 0.5–1 × 10^6 TU in 2 μl (equivalent to 150 ng of p24 protein for bicistronic viruses, 70–80 ng of p24 for monocistronic viruses).

Mice. β2KO mice were back-crossed to the C57BL/6J@Ico strain for 19 generations. All mice used in this work were kept under standard laboratory conditions with ad libitum food and water and in a 12-h light/dark period (on at 8:00 a.m.).

Stereotaxic Procedure. Mice aged 8–10 weeks (weight 25–30 g) were anesthetized by using ketamine/xylazine and introduced into a stereotaxic frame adapted for mice. Two microliters of virus were injected bilaterally for SNpc at the following coordinates (34): antero-posterior: −3.0 mm (from bregma), lateral ± 1.3 mm, and dorso-ventral −4.3 mm from the skull. For VTA injections, the coordinates were: −3.5 mm antero-posterior, ± 0.5 mm lateral, and −4.4 mm dorso-ventral. All procedures were in accordance with European Commission directives 219/1990 and 220/1990 and approved by Animalerie Centrale and Médecine du Travail, Institut Pasteur.

[^{125}I]-Epibatidine Autoradiography. To determine the presence of high-affinity nicotinic β2*-nAChRs sites, brains were dissected, frozen in dry ice, and stored at −80°C until use. Twenty-micron-thick coronal sections were cut at −20°C and thawed mounted on Menzel Gläser SuperFrost Plus microscope slides. Slides were incubated at room temperature with 200 pM [^{125}I]-epibatidine (NEN Perkin-Elmer; specific activity 2,200 Ci/mmol) in 50 mM Tris (pH 7.4) for 30 min. After incubation, sections were rinsed 2 × 5 min in the same buffer and briefly in distilled water. Nonspecific binding was not distinguishable from background. Sections were exposed for 24–8 h to Kodak Biomax films. As previously reported (19), high-affinity [^{125}I]-epibatidine binding sites were absent from the brain of β2 knockout mice, with the exception of structures of the habenulo-peduncular system (including the interpeduncular nucleus and the fasciculus retroflexus), strongly labeled because of the abundance of high-affinity nicotinic β4*-nAChRs sites.

***In Vivo* Microdialysis (Basal DA Release).** Mice were anesthetized with an i.p. injection of a ketamine/xylazine mixture (5:1; 0.10 ml/10 g) and placed in a stereotaxic apparatus. A guide cannula (CMA7, CMA Microdialysis) was implanted vertically in the striatum [AP, +0.6; ML, ± 1.8; DV, −2.5 mm from bregma (34)] and then fixed to the skull with dental cement. Forty-eight hours later, an analytical probe (CMA7/2 mm, CMA Microdialysis) was inserted into the cannula under light anesthesia (2% isoflurane). Twenty-four hours after probe insertion, animals were habituated to the microdialysis environment overnight with food and water ad libitum. The next morning, probes were perfused with a Ringer solution [148 mM NaCl, 2.7 mM KCl, 1.2 mM $CaCl_2$, and 0.8 mM $MgCl_2$, (pH 6.0)] at a constant rate of 1 μl/min, and five baseline samples were taken every 20 min. Mice were challenged with an injection of saline (0.1 ml/10 g, i.p.), and the collection of samples continued for another hour. Dialysates (20 μl) were injected directly into a HPLC system, consisting of a pump linked to an automatic injector (Agilent 1100), a reverse-phase column (Zorbax SB C18, 5 μm, 150 × 4.6 mm, Agilent Technologies), and a coulometric detector (Coulochem II, ESA Inc.) with a 5011A analytical cell. DA was quantified as previously described (35). Briefly, the first electrode was fixed at −100 mV and the second electrode at +300 mV. The gain of the detector was set at 10 nA. The composition of the mobile phase was 50 mM NaH_2PO_4, 0.1 mM Na_2EDTA, 0.65 mM octyl sodium sulfate, and 15% (vol/vol) methanol (pH 3.5). The flow rate was set at 0.9 ml/min, and the sensitivity of the assay for DA was 1 pg/20 μl.

Behavioral Experiments: ***Open field.*** Mice were placed in the center of an empty 100-cm-diameter circular arena, and their trajectories were recorded for 30 min. The experiment was performed under a soft illumination (10 lux) during the light period (between 11:00 a.m. and 4:00 p.m.). A camera, fixed to the ceiling above the open field, was connected to the videotrack system (Viewpoint) out of sight of the animals. This videotrack was used to determine total distance traveled and to record the time spent either in fast movements (speed ≥ 11.8 cm/sec) or slow movements (speed ≤ 6.25 cm/sec).

Activity over 24 h. To evaluate their activity rhythm during 24 h, mice were placed individually into four wide transparent boxes (50 × 50 × 50 cm) covered with sawdust, with free access to food and water as in home cages. They were maintained in the usual light/dark cycle by an automatic control device connected to lamps. The dark phase started at 8:00 pm and stopped at 8:00 a.m. A video-camera fixed to the ceiling out of sight of the animals and connected to the videotrack system (View-point) was used to record their movements in intervals of 30 min during the 24-h test. Activity analysis was expressed as total distance traveled in each of the 48 intervals.

Statistical analyses. All data were analyzed either by one-way ANOVA, two-way ANOVA, or repeated-measures ANOVA, followed by post hoc tests as indicated. In some cases, the two-tailed Student's *t* test was performed as indicated.

ACKNOWLEDGMENTS. We thank Martine Soudant and Anne Cormier for excellent technical assistance; Pavel Osten for providing pCMV-U6 and FUG-Wlinker plasmids; Juan Ferrario for help with images; and Marcelo Rubinstein, Morgane Besson, Nadine Kabbani, and Ines Ibanez-Tallon for comments on the manuscript. M.E.A. acknowledges financial support from Fondation pour la Recherche Médicale and Région Ile-de-France. This work was supported by Institut Pasteur, Unité de Recherche Associée 2182, Centre National de la Recherche Scientifique, Collège de France, Association pour la Recherche sur le Cancer, and the French National Science Foundation Grant ANR ''Neuroscience, Neurologie et Psychiatrie 2005'' (to U.M.), Fondo de Investigaciones Sanitarias Grant PI070709 (to P.R.), and Ministerio de Ciencia y Tecnología SAF2007-64062 (to R.M.).

1. Carlsson A (1993) Thirty years of dopamine research. *Adv Neurol* 60:1–10.
2. Everitt BJ, Robbins TW (2005) Neural systems of reinforcement for drug addiction: From actions to habits to compulsion. *Nat Neurosci* 8:1481–1489.
3. Goldman-Rakic PS (1998) The cortical dopamine system: Role in memory and cognition. *Adv Pharmacol* 42:707–711.
4. Ungerstedt U (1971) Stereotaxic mapping of the monoamine pathways in the rat brain. *Acta Physiol Scand Suppl* 367:1–48.
5. Carlsson A (1972) Biochemical and pharmacological aspects of Parkinsonism. *Acta Neurol Scand Suppl* 51:11–42.
6. Bolam JP, Francis CM, Henderson Z (1991) Cholinergic input to dopaminergic neurons in the substantia nigra: A double immunocytochemical study. *Neuroscience* 41:483–494.
7. Smith AD, Bolam JP (1990) The neural network of the basal ganglia as revealed by the study of synaptic connections of identified neurones. *Trends Neurosci* 13:259–265.
8. Floresco SB, West AR, Ash B, Moore H, Grace AA (2003) Afferent modulation of dopamine neuron firing differentially regulates tonic and phasic dopamine transmission. *Nat Neurosci* 6:968–973.
9. Blaha CD, *et al.* (1996) Modulation of dopamine efflux in the nucleus accumbens after cholinergic stimulation of the ventral tegmental area in intact, pedunculopontine tegmental nucleus-lesioned, and laterodorsal tegmental nucleus-lesioned rats. *J Neurosci* 16:714–722.
10. Blaha CD, Winn P (1993) Modulation of dopamine efflux in the striatum following cholinergic stimulation of the substantia nigra in intact and pedunculopontine tegmental nucleus-lesioned rats. *J Neurosci* 13:1035–1044.
11. Zhou FM, Wilson CJ, Dani JA (2002) Cholinergic interneuron characteristics and nicotinic properties in the striatum. *J Neurobiol* 53:590–605.
12. Saka E, Iadarola M, Fitzgerald DJ, Graybiel AM (2002) Local circuit neurons in the striatum regulate neural and behavioral responses to dopaminergic stimulation. *Proc Natl Acad Sci USA* 99:9004–9009.
13. Klink R, de Kerchove d'Exaerde A, Zoli M, Changeux JP (2001) Molecular and physiological diversity of nicotinic acetylcholine receptors in the midbrain dopaminergic nuclei. *J Neurosci* 21:1452–1463.
14. Champtiaux N, *et al.* (2003) Subunit composition of functional nicotinic receptors in dopaminergic neurons investigated with knock-out mice. *J Neurosci* 23:7820–7829.
15. Mameli-Engvall M, *et al* (2006) Hierarchical control of dopamine neuron-firing patterns by nicotinic receptors. *Neuron* 50:911–921.
16. Zhou FM, Liang Y, Dani JA (2001) Endogenous nicotinic cholinergic activity regulates dopamine release in the striatum. *Nat Neurosci* 4:1224–1229.
17. Luetje CW, Patrick J, Seguela P (1990) Nicotine receptors in the mammalian brain. *FASEB J* 4:2753–2760.
18. Court JA, Perry EK (1995) Distribution of nicotinic receptors in the CNS. In *CNS Neurotransmitters and Neuromodulators*: *Acetylcholine* (CRC Press, Boca Raton, FL).
19. Picciotto MR, *et al.* (1995) Abnormal avoidance learning in mice lacking functional high-affinity nicotine receptor in the brain. *Nature* 374:65–67.
20. Picciotto MR, *et al.* (1998) Acetylcholine receptors containing the β2 subunit are involved in the reinforcing properties of nicotine. *Nature* 391:173–177.
21. Granon S, Faure P, Changeux JP (2003) Executive and social behaviors under nicotinic receptor regulation. *Proc Natl Acad Sci USA* 100:9596–9601.
22. Maskos U, *et al.* (2005) Nicotine reinforcement and cognition restored by targeted expression of nicotinic receptors. *Nature* 436:103–107.
23. Day J, Damsma G, Fibiger HC (1991) Cholinergic activity in the rat hippocampus, cortex and striatum correlates with locomotor activity: An in vivo microdialysis study. *Pharmacol Biochem Behav* 38:723–729.
24. Fountaine TM, Wood MJ, Wade-Martins R (2005) Delivering RNA interference to the mammalian brain. *Curr Gene Ther* 5:399–410.
25. Davids E, Zhang K, Tarazi FI, Baldessarini RJ (2003) Animal models of attention-deficit hyperactivity disorder. *Brain Res Brain Res Rev* 42:1–21.
26. Tang K, Low MJ, Grandy DK, Lovinger DM (2001) Dopamine-dependent synaptic plasticity in striatum during in vivo development. *Proc Natl Acad Sci USA* 98:1255–1260.
27. Maskos U (2008) The cholinergic mesopontine tegmentum is a relatively neglected nicotinic master modulator of the dopaminergic system: Relevance to drugs of abuse and pathology. *Brit J Pharmacol* 153:S438–S445.
28. Hirsch EC (2000) Nigrostriatal system plasticity in Parkinson's disease: Effect of dopaminergic denervation and treatment. *Ann Neurol* 47:S115–120.
29. Quik M (2004) Smoking, nicotine and Parkinson's disease. *Trends Neurosci* 27:561–568.
30. Castellanos FX, Tannock R (2002) Neuroscience of attention-deficit/hyperactivity disorder: The search for endophenotypes. *Nat Rev Neurosci* 3:617–628.
31. Granon S, Changeux JP (2006) Attention-deficit/hyperactivity disorder: A plausible mouse model? *Acta Paediatr* 95:645–649.
32. Coger RW, Moe KL, Serafetinides EA (1996) Attention deficit disorder in adults and nicotine dependence: Psychobiological factors in resistance to recovery? *J Psychoactive Drugs* 28:229–240.
33. Yuan B, Latek R, Hossbach M, Tuschl T, Lewitter F (2004) siRNA Selection Server: An automated siRNA oligonucleotide prediction server. *Nucleic Acids Res* 32:W130–134.
34. Paxinos G, Franklin KBJ (2001) *The Mouse Brain in Stereotaxic Coordinates* (Academic, San Diego).
35. Robledo P, *et al.* (2004) The rewarding properties of MDMA are preserved in mice lacking mu-opioid receptors. *European J Neurosci* 20:853–858.